Journal of Geochemical Exploration 154 (2015) 252–264

Contents lists available at ScienceDirect

Journal of Geochemical Exploration

journal homepage: www.elsevier.com/locate/jgeoexp

Multifractal modelling-based mapping and identification of geochemical anomalies associated with Cu and Au mineralisation in the NW Junggar area of northern Xinjiang Province, China

Feng Yuan [a,*], Xiaohui Li [a,b], Taofa Zhou [a], Yufeng Deng [a], Dayu Zhang [a], Chao Xu [a], Ruofei Zhang [a], Cai Jia [a], Simon M. Jowitt [c]

[a] School of Resources and Environmental Engineering, Hefei University of Technology, Hefei 230009, China
[b] Centre for Exploration Targeting, University of Western Australia, Crawley 6008, Western Australia, Australia
[c] School of Geosciences, Monash University, Clayton, VIC 3800, Australia

ARTICLE INFO

Article history:
Received 8 January 2014
Revised 24 November 2014
Accepted 26 November 2014
Available online 10 December 2014

Keywords:
Geochemistry
Singularity
Multifractal models
NW Junggar
China

ABSTRACT

The NW Junggar area is located within the north of Xinjiang Province, China, and hosts several recently discovered hydrothermal copper and gold deposits. The presence of these deposits and the relatively unexplored nature of this area means that the NW Junggar region can be considered highly prospective. This study focuses on the identification of mineralisation-related As, Cu and Au soil geochemistry anomalies within the area using a combined singularity mapping, multifractal kriging and spectrum–area (S–A) fractal modelling approach. The approach utilises an optimised version of the singularity mapping technique and outlines details of the use of a S–A fractal modelling approach for the precise identification of individual geochemical anomalies. This modelling and anomaly identification was ground-truthed by field reconnaissance, leading to the identification of mineralisation associated with anomalies determined using fractal and multifractal modelling in the study area. This successful ground-truthing, and the identification of mineralised areas using the techniques outlined here, indicate that this approach could be a useful tool in further geochemcial exploration and research, both in the NW Junggar area and in other areas that host similar Cu and Au deposits.

1. Introduction

Exploration geochemistry is an important method in mineral exploration targeting and the determination of the prospectivity of an area during mineral exploration. This is especially true of areas that are relatively unexplored, as potential mineralisation-related geochemical anomalies can be rapidly delineated, meaning that exploration geochemistry data can be used as a guide for targeting areas for more detailed exploration (Bonham-Carter, 1994; Carranza, 2009; Pan and Harris, 2000; Wang et al., 2011). In addition, these delineated anomalies can efficiently be used in more advance exploration-focused modelling, such as GIS-based prospectivity mapping (Bonham-Carter, 1994; Carranza, 2009; Pan and Harris, 2000; Wang et al., 2011).

The majority of previous studies of exploration geochemical data have used classical statistical approaches, such as the construction of probability graphs using frequency distributions and correlation-based univariate and multivariate analysis (Carranza, 2009; Zuo, 2011a; Zuo et al., 2012). These classical statistical approaches generally focus on the frequency distribution of elemental concentrations and the correlations between multiple variables (Zuo et al., 2009), with subsequent geostatistical and kriging-based modelling, allowing the analysis of spatial structures and the spatial characteristics of exploration geochemical data by the identification of spatial trends and variations by interpolation. However, this interpolation almost invariably leads to the smoothing-out of anomalous values. This is a significant problem in mineral exploration and prospectivity modelling, where these anomalies may well be high-priority exploration targets. In addition, anomalous often overlap with background, or weak anomalies are hidden within the strong variance of background (Cheng, 2007; Zuo and Cheng, 2008). Background concentrations of elements of interest for Cu–Au mineralisation and pathfinder elements, such as Au, Cu and As, have high variances as a result of multiple geological processes (Zuo, 2011a), meaning that the efficient extraction and identification of anomalies are a key process during the interpretative statistical treatment of exploration geochemistry data (Zuo et al., 2009).

Recent research has identified that the release of energy or the accumulation of mass during various geological processes, such as volcanic eruptions, occurs within narrow intervals in time or space, leading to the formation of geological anomalies (Cheng, 2008a; Cheng and Agterberg, 2009). These anomalies can also be termed singularities, and the geological processes that form them are termed singular

* Corresponding author. Tel.: +86 55162901648.
E-mail address: yf_hfut@163.com (F. Yuan).

http://dx.doi.org/10.1016/j.gexplo.2014.11.015
0375-6742/

processes (Cheng, 1999, 2007, 2012). These singular processes always result in fractality and multifractality, primarily due to the natural non-linear attributes involved in these processes (Cheng, 2007, 2008b; Cheng and Agterberg, 2009). Recent advances in the methods used in fractal and multifractal analysis have included the development of singularity mapping techniques, multifractal interpolation models, and spectrum–area (S–A) fractal models, all of which have been used to separate and identify geochemical anomalies (Cheng, 2007; Cheng and Agterberg, 2009; Cheng et al., 2010; Yuan et al., 2012; Zuo et al., 2009). These models cannot only be used to describe the fractal and multifractal characteristics of geochemical data, but can also be used to identify more effectively strong and weak anomalies from complex geochemical background data. Here, a case study using geochemical data from the NW Junggar area of China is presented.

The NW Junggar area is located in the north-west of Xinjiang Province, China, in an area of continental dry climate with an average annual rainfall of 291 mm (Fig. 1a). This combination of low rainfall and dry climate means this area is sparsely vegetated; where present, this vegetation is dominated by plants acclimatised to arid regions. This area is sparsely populated, and the industry of this area is dominated by animal husbandry, with few people involved in agriculture and/or mining.

Several copper and gold deposits have been discovered in the study area. Although this area has only undergone minimal exploration, meaning that the area should be considered highly prospective for future mineral exploration and the discovery of copper and gold deposits. Here, the focus is on the NW Junggar area, and the use of both fractal and multifractal modelling approaches, using As, Cu and Au soil geochemical data to identify geochemical anomalies related to known Cu and Au mineralisation, and to identify highly prospective areas with no currently known mineralisation. A number of these highly prospective areas were also visited to ground-test the results of the geochemical data analysis, directly leading to the discovery of new areas of mineralisation, and verifying the usefulness of this fractal and multifractal modelling during mineral exploration in the NW Junggar area and elsewhere.

2. Geology and mineralisation

The NW Junggar area is located in the north-west of Xinjiang Province, China, within the southwestern Central Asian Orogenic Belt (Fig. 1a). The area is divided into the Sawuer–Taerbahatai and Xiemisitai sub-regions (Fig. 1b).

The region is dominated by structures developed during NE–SW and E–W extension, with the latter associated with the development of the Sawuer, Taerbahatai and Hongguleleng faults in addition to numerous faults and folds in the north of the area. The study area to the south of the Hongguleleng Fault also contains ENE–WSW-oriented faults that dip to the NW, and all major faults are associated with well-developed subsidiary fractures, with varying spatial and temporal characteristics indicative of multiple phases of faulting. These structures play an important role in controlling outcropping lithologies, magmatism, and the type and location of mineralisation in the study area (Chen et al., 2010; Shen et al., 2007).

The study area contains Palaeozoic pyroclastic, volcaniclastic sedimentary and volcanic rocks, and widespread intrusive rocks of ultramafic to felsic composition, although the majority of these intrusions are of felsic composition (Fan et al., 2007; Zhou et al., 2006). These intrusions are present as batholiths and stocks, in addition to apophyses and dykes, and the majority of these intrusions are of diorite, quartz diorite, granodiorite, monzogranite and alkali granite composition (Jahn et al., 2000; Zhou et al., 2006).

The NW Junggar area is adjacent to the Salma–Sawuer metallogenic belt and the Genghis–Tarbaghatai metallogenic belt of Kazakhstan (Shen et al., 2007). These metallogenic belts host the Chaersike magmatic chromite, the South Makesute magmatic copper–nickel sulphide, and the Kezierkayin and Kensai porphyry copper deposits, in addition to numerous volcanic sediment-hosted polymetallic copper deposits, and disseminated and quartz vein-type gold, tungsten, mercury, and auriferous sulphide deposits. In comparison, only a few mineral deposits have been exposed in the continuation of these two metallogenic belts

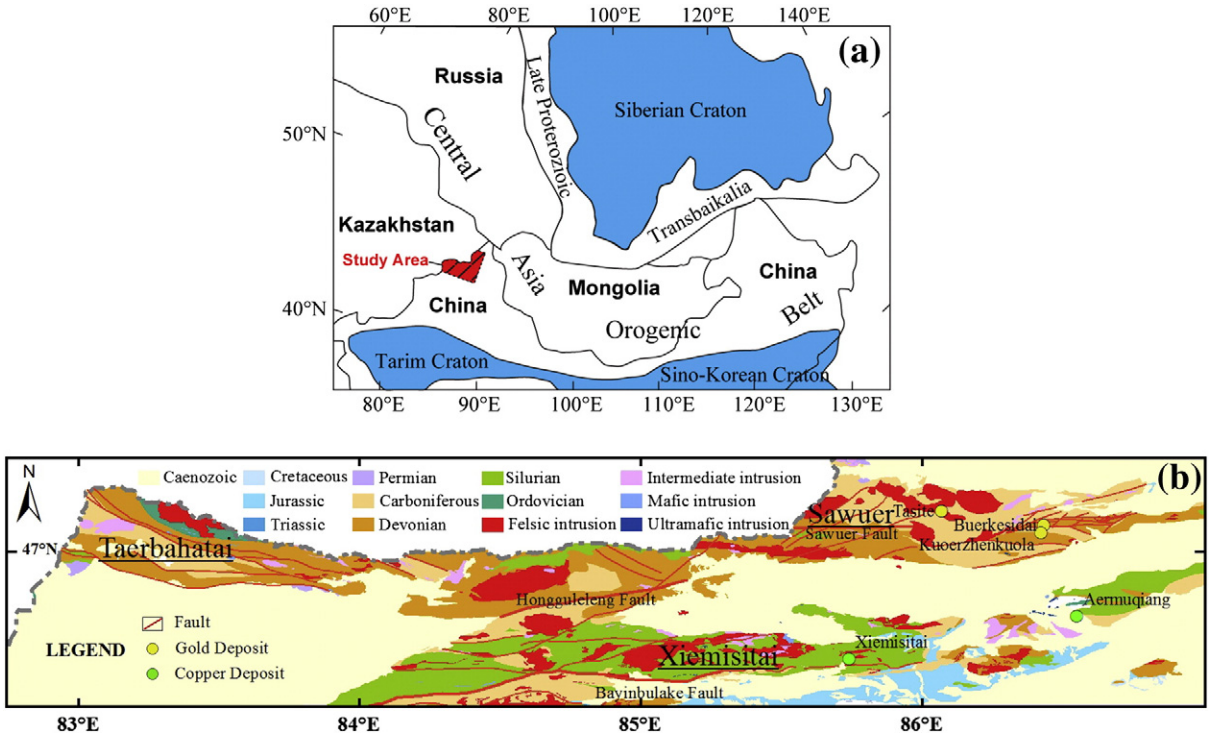

Fig. 1. (a) Map showing the location of the study area within the north of Xinjiang Province in an area dominated by the Central Asia Orogenic Belt (modified after Jahn et al., 2000); (b) Simplified geological map of the NW Junggar area, showing major faults and Au and Cu deposits in the study area (modified after BGMRXUAR, 1993).

within China, including the Aermuqiang and Xiemisitai copper deposits, and the Quoerzhenkuola, Buerkesidai and Tasite gold deposits (Fig. 1b). This indicates that the NW Junggar area should be considered highly prospective for future mineral exploration.

Among the discovered deposits in the study area, the Kuoerzhenkuola and Buerkesidai gold deposits are the two largest volcanic-hosted gold deposits. They are hosted in a caldera structure consisting of volcanic and subvolcanic rocks, and controlled by a caldera fracture system overprinted by regional faults. The host rocks are mainly andesite in the Kuoerzhenkuola deposit, and carbonaceous silty tuff in the Buerkesidai deposit, respectively. Numerous researchers have studied the characteristics and genesis of these two deposits, and have proposed various models (Guo, 1997; Wang et al., 2004; Yin et al., 1996). After further studies on geology, geochemistry and geochronology, Shen et al. (2007) proposed that these two volcanic-hosted gold deposits share the same genesis, and are both classified as volcanogenic hydrothermal gold deposits. There have been only a few studies on Xiemisitai and Aermuqiang copper deposits, and Shen et al. (2010) proposed that Xiemisitai copper deposits should be classified as of hydrothermal origin.

3. Data

A total of 2854 topsoil samples were collected over a 2 by 2 km grid within the study area, out of which 3–5 samples were composited into one sample. These soil samples overlie Palaeozoic units and intrusions and the locations of these samples are shown in Fig. 2.

The concentrations of a total of 39 major and trace elements were measured during this study. Here, the concentrations of As, Cu and Au within these soil samples are considered, and they are used in the identification of anomalies associated with known Cu and Au mineralisation. Arsenic was determined by hydride generation-atomic fluorescence spectrometry (HG-AFS), Au by graphite furnace atomic absorption spectrophotometry (GF-AAS), and Cu by inductively coupled plasma mass spectrometry (ICP-MS).

A statistical treatment of the data was undertaken and the summary results are shown in Table 1. The concentrations of As, Cu and Au are highly spatially variable and have high skewness and kurtosis values, indicating that these data sets contain outliers and are non-normally distributed (Fig. 3). These data are also positively skewed; this is especially apparent in the Au data that have the highest skewness and kurtosis coefficients, and the highest number of outlying data points.

4. Multifractal modelling

In order to identify more reliably, and to separate strong and weak anomalies associated with known Cu and Au mineralisation, the singularity mapping technique and S–A fractal modelling approach were used on the concentrations of As, Cu and Au.

Table 1
Statistical analysis of soil geochemical data from study area.

Element	Concentration						CV*
	Min	Max	Mean	Standard deviation	Skewness	Kurtosis	(%)
As (mg/kg)	0.28	333	14.85	14.74	7.12	109.40	99.25
Cu (mg/kg)	4	222	37.78	18.32	2.24	14.29	48.52
Au (μg/kg)	0.1	370	1.35	7.55	43.07	2028.16	559.64

* CV: Coefficient of Variation.

4.1. Singularity mapping technique

Singularity mapping is a technique used to identify geochemical anomalies that result from singular processes (Cheng, 2007; Zuo and Cheng, 2008; Zuo et al., 2009, 2015–in this issue). These singularities can be estimated using a sliding window method that uses the following formula to define the relationship between the average element concentration and the size of the window:

$$X = c \cdot \varepsilon^{E-\alpha}$$

where X is the average concentration, c is a constant value, α is the singularity, ε is the size of the window, and E is the Euclidean dimension (Agterberg, 2012). These techniques are still using, however, Euclidean properties, and they have not yet been adapted to Compositional Data Analysis (CoDA), as geochemical data are compositional, because they comprise strictly positive components, which sum up to a constant, e.g., 1,000,000 mg/kg or 100 wt.% (Aitchison, 1986; Filzmoser et al., 2009, 2010, 2014; Egozcue and Pawlowsky-Glahn, 2011; Reimann et al., 2012; Buccianti, 2015–in this issue; Sadeghi et al., 2015–in this issue).

Singularity estimation can use either raw or gridded geochemical data after interpolation. The method uses the following steps: (1) defining a set of sliding windows $A(r)$ with both variable and identical interval window sizes, $r_{min} = r_1 < r_2 < \ldots < r_n = r_{max}$; this approach generally uses square window shapes; (2) calculating the singularity at all locations within the study area during steps (3) and (4); (3) calculating the average concentration $C[A(r_i)]$ obtained for each size of window; and (4) plotting the average concentration $C[A(r_i)]$ against the size of the window r used to obtain that average concentration on a log–log graph, which should theoretically show a linear relationship (Zuo et al., 2013):

$$\log C[A(r_i)] = c + (2-\alpha)\log(r).$$

The singularity value α can be estimated using a linear fitting method from the log–log relationship defined using steps (1)–(4) above. An α value close to 2 indicates that the given location does not have the characteristics of singularity, whereas locations with values >2 are indicative of areas with element concentration enrichment, and

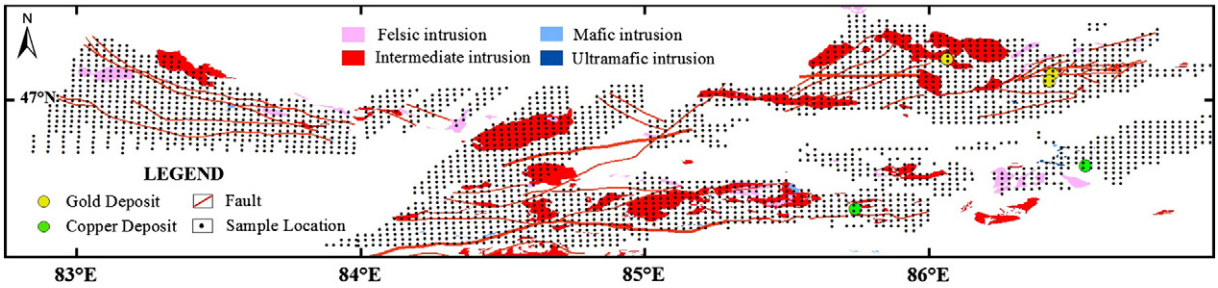

Fig. 2. Location map of soil samples, NW Junggar area of northern Xinjiang Province, China.

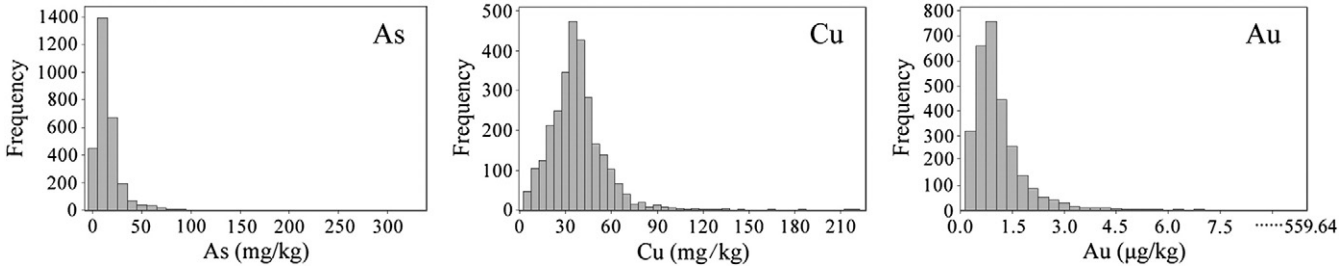

Fig. 3. Histograms showing the distribution of As, Cu and Au within the data set used in this study.

locations with values <2 are indicative of areas with depleted element concentration (Cheng, 2007; Zuo et al., 2013).

However, this use of a log–log plot and linear fitting method to identify singularities generally has some data points that deviate from a single straight line, meaning that this approach using a single straight line may not accurately model all data points (Zuo et al., 2013) (Fig. 4), indicating that these data may have multifractal characteristics. In order to estimate more accurately the location of singularities, this approach uses the following steps to optimise singularity estimation:

(1) Plotting window size and corresponding element concentration data points on a log–log graph.
(2) Using a least squares method to fit the first three data points from the smallest window size, and then increasing the window size and calculating the fitting coefficient R^2. This initial calculation is then followed by more calculations with increased window sizes and again using a least squares method to fit the data points relating to windows smaller than the largest window size, and again calculating R^2 fitting coefficients.
(3) Selecting the data point sets with the highest R^2 values, and fitting a single straight line through these data points.
(4) Steps 2 and 3 are then repeated starting from the data point adjacent to the data point sets above to obtain another straight line until all of data points fit to a single straight line.
(5) The final step is to select a single straight line to calculate singularity values relating to the main research aim.

The original approach using a single straight line to fit all data points yields a poor fitting coefficient R^2 value of 0.5004, meaning that it is hard to use a single straight line to fit all data points. However, using the piecewise linear fit method, outlined above, means that all data points can be fitted using two straight lines, yielding fitting coefficient R^2 values close to 1 (Fig. 4).

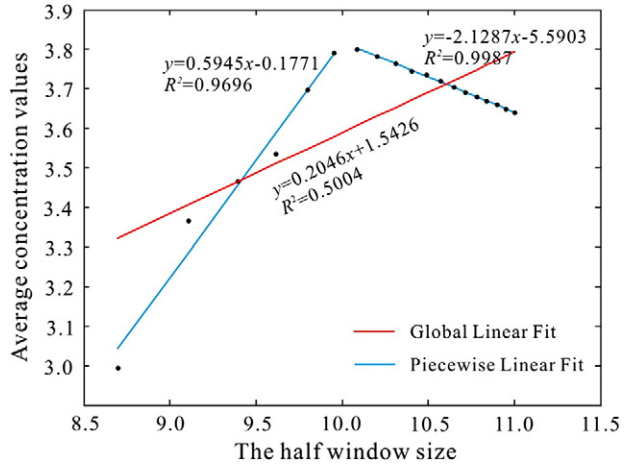

Fig. 4. Log–log plot with fitted linear correlation lines showing the relationship between the half window size (r) versus average concentrations $C[A(r_i)]$.

These fitting results indicate that the distribution of data in this area has two different scale independent ranges. The small range represents depleted element concentrations, whereas the larger range represents enriched element concentrations. The fact that the anomaly analysis, undertaken during this study, is focused on the identification of local geochemical anomalies, means that the first straight line defined during the piecewise linear fit modelling outlined above is used to calculate the location of singularities.

The results of the global linear and piecewise linear fit methods, both identify data with depleted element concentrations, although these data are more clearly identified using the piecewise linear fit method. The other straight line fit, obtained using the piecewise linear fit method, can also be used for research into the larger-scale magmatism and ore-forming processes that control the concentrations of the elements of interest in this area.

4.2. Multifractal kriging interpolation

Cheng (1999) proposed a multifractal interpolation method using singularity and moving average interpolation to simultaneously measure local singularities and the spatial correlation between data, whilst also overcoming the smoothing effect of applying a moving average interpolation method. The key principle of this method is the addition of a singularity value to the moving average interpolation method as follows:

$$Z(x_0) = \varepsilon^{\alpha(x_0)-2} \sum_{\Omega(x_0,\varepsilon)} \omega(\|x-x_0\|)Z(x)$$

where $\alpha(x_0)$ is a singularity at location x_0, and ω is the weight of the moving average function. If x_0 is located in an area with normal or background concentrations, for a 2D data set, $\alpha(x_0) = 2$, meaning that the multifractal interpolation method outlined above will give a value equal to the moving average interpolation method. In comparison, if x_0 is located in an area of greater than average element concentrations (i.e., areas of enrichment), which contain local singularity characteristics and have $\alpha(x_0)$ values >2, the multifractal interpolation method will give a larger value than the moving average interpolation method, and if x_0 is located in an area of lower than average element concentrations (i.e., areas of depletion) with $\alpha(x_0)$ values <2, the multifractal interpolation method above will yield values lower than those obtained using the moving average interpolation method.

Multifractal interpolation cannot only convert point data to a continuous surface, but also it can retain the local spatial structure and singularity during this interpolation (Cheng, 2001a). This approach has also proven to be useful in mineral exploration, and the interpretation of exploration geochemistry data (Lima et al., 2003; Cheng, 2008c; Zuo, 2011b; Yuan et al., 2012).

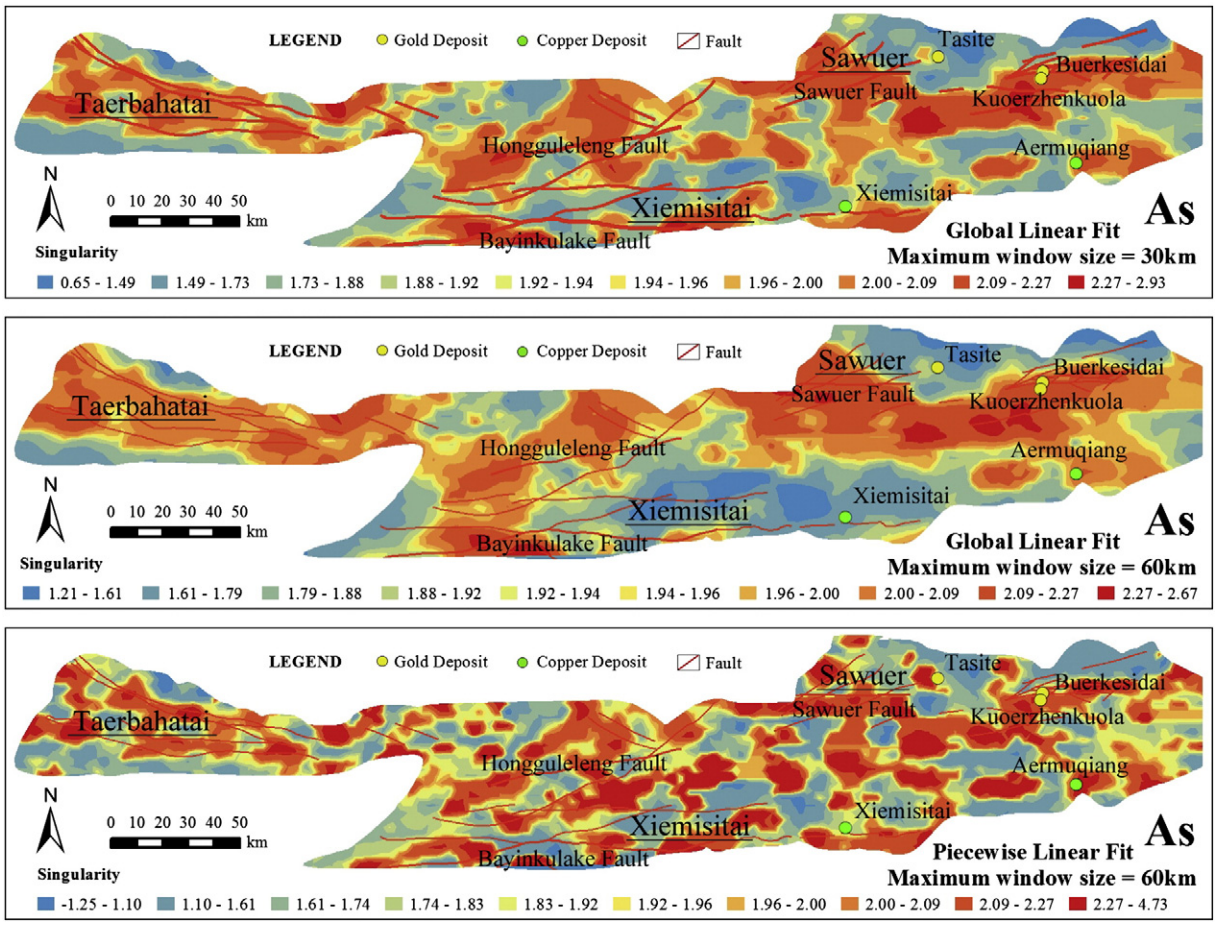

Fig. 5. Maps showing the location of As singularities using global linear and piecewise linear fitting methods and different maximum window sizes of 30 and 60 km, NW Junggar area of northern Xinjiang Province, China.

Ordinary Kriging (Krige, 1951; Matheron, 1963; Isaaks and Srivastava, 1990; Journel and Huijbreghts, 1978) is a best linear unbiased estimator for spatial data (Clark, 1979; Clark and Harper, 2007) that uses a moving average approach to interpolate between individual points. Although this approach leads to smoothing of the data, ordinary Kriging can effectively determine the spatial variability within a data set

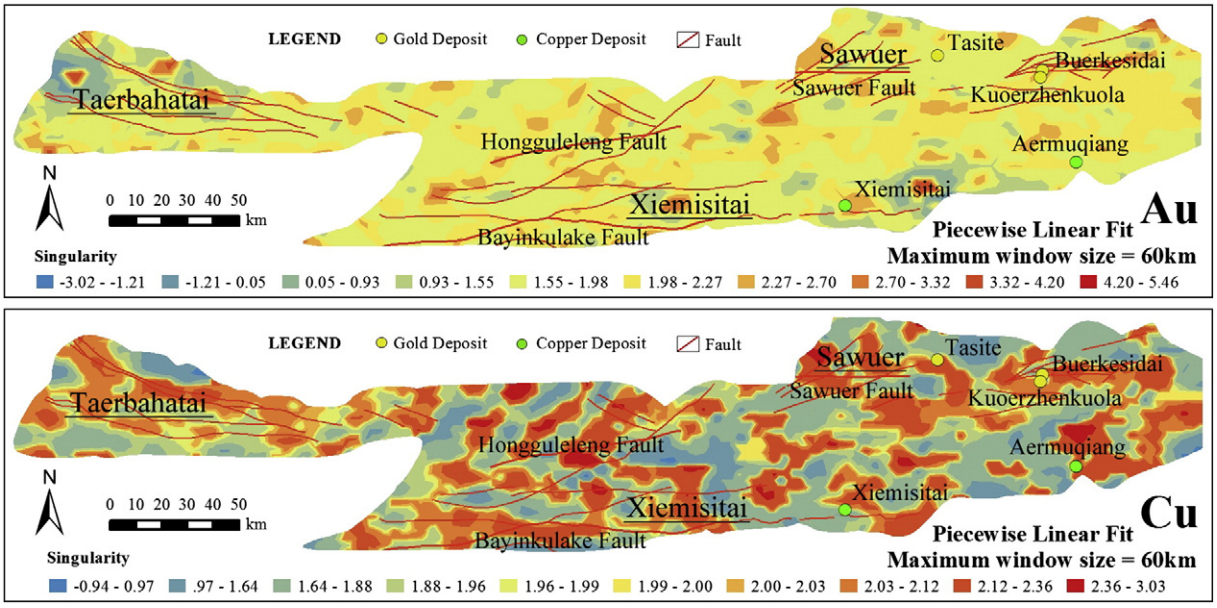

Fig. 6. Maps showing the location of Au and Cu singularities determined by piecewise linear fitting methods and a maximum window size of 60 km, NW Junggar area of northern Xinjiang Province, China.

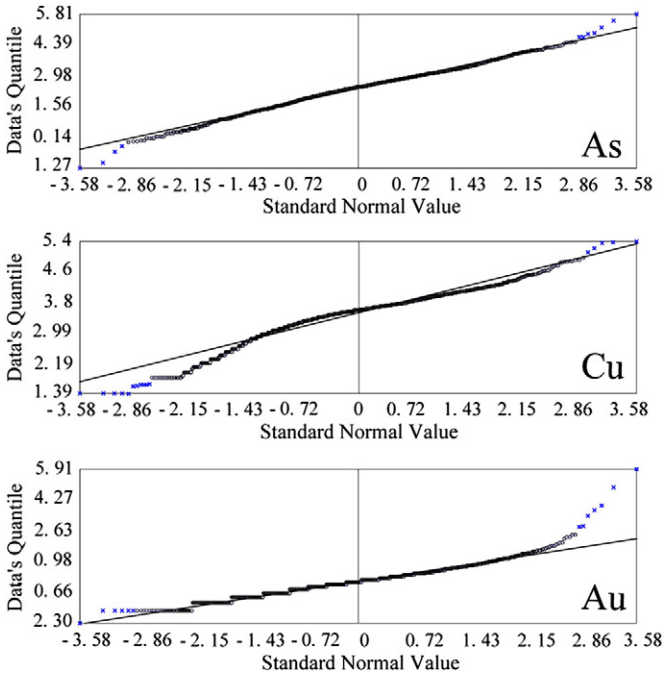

Fig. 7. Logarithmic Q–Q plot showing the distribution of As, Cu and Au data points within the soil geochemical data set used in this study; blue points indicate the outliers that were removed prior to interpolation.

using variogram models to extract the necessary kriging parameters for plotting a raster map (Zhang, 2005).

A more advanced approach is offered by multifractal kriging, a method that integrates both kriging and multifractal interpolation methods. This approach analyses the multifractal characteristics of the data set being considered, meaning that the data can be rectified using singularity values and, therefore, combines the advantages of both kriging and multifractal interpolation methods (Li, 2005).

4.3. Spectrum–area fractal modelling

Spectrum–area (S–A) fractal modelling is based on generalised self-similarity theory (Cheng, 2006a); this approach determines the fractal characteristics of a data set by converting spatial data to frequency domain data. This fractal modelling approach is an extension of the frequency domain-based Concentration–Area (C–A) modelling (Cheng et al., 1994; Zuo et al., 2013). This generalised self-similarity modelling approach determines the relationship between spectral energy density values greater than S (spectral energy density), and the area covered by sets of data that have wave number attributes greater than S [$A(>S)$] within a 2D frequency domain, using the following formula (Cheng et al., 2000; Cheng, 2001b, 2006b):

$$A(\geq S) \propto S^{-2d/\beta}$$

where β is the anisotropic scaling exponent, d is a parameter representing the degree of overall concentration, and $\propto$ denotes

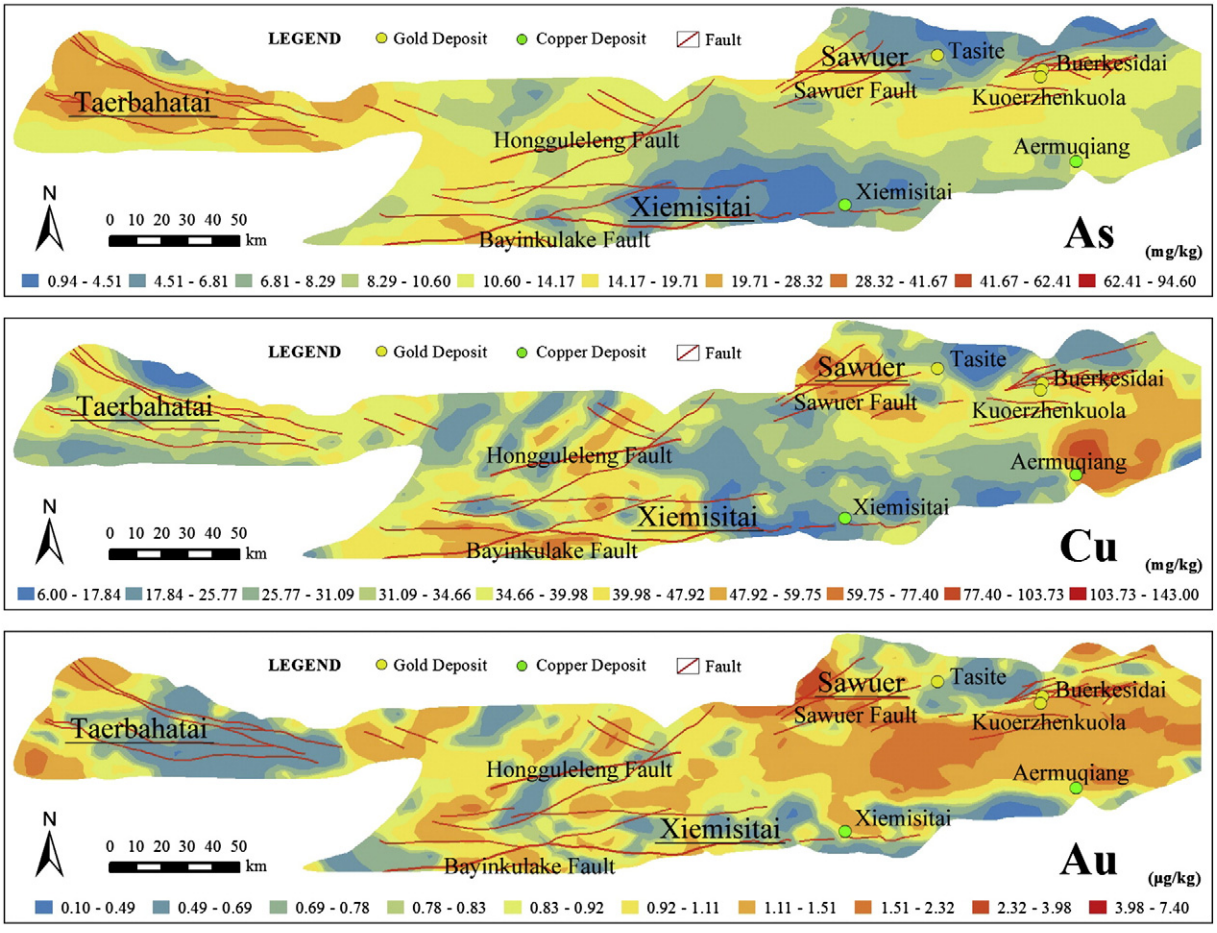

Fig. 8. Maps showing the spatial distribution of As, Cu and Au in the study area; these maps were produced by lognormal kriging interpolation, NW Junggar area of northern Xinjiang Province, China.

proportionality (Zuo et al., 2013). Rearranging this formula for use with 2D data gives the following:

$$A(\geq S) \propto S^{-2d}.$$

The differing self-similarity characteristics within the frequency domain means that two different filters can be used to separate background and anomalous concentrations, here termed the background and anomaly filters.

Most recent research has used S–A fractal modelling to separate geochemical anomalies from background concentrations (e.g. Cheng et al., 2010; Zuo, 2011a, 2011b; Zuo et al., 2012, 2013). This approach uses several steps (Zuo et al., 2013), which are outlined below:

(1) Multifractal interpolation to interpolate geochemical data to generate a raster map;
(2) Fourier transformation to convert the raster map into frequency domain data;
(3) Plotting of spectral energy density (S) against the areas of sets of data with wave number values $> S$ on a log–log graph, and using the least squares method to fit ($N \geq 2$) straight lines to these data.
(4) Estimation of cut-off values by calculating the intersection between the ($N \geq 2$) straight lines, with the lower cut-off value used to define the anomaly filter, and the higher cut-off value used to define the background filter;
(5) The anomaly and background filters defined in step 4 are then used to filter the frequency domain data before inverse Fourier transformation to convert these frequency domain data back to spatial domain data. A geochemical distribution map showing the location of areas with background and anomalous concentrations is then constructed.

5. Results of analysis and discussion

5.1. Singularity mapping

Singularities can be identified using both raw and gridded data that are interpolated from the raw data. Gridding of raw data can enable more detailed visualisation of the spatial characteristics of the data and can improve singularity identification, especially in areas with infrequent sampling or with large sample spacing. However, interpolation generally uses a moving average method, meaning that areas with anomalously high concentrations are smoothed, potentially occluding anomalous areas and making anomaly identification difficult.

The data used in this study were obtained at a high sampling density, meaning that it is possible to use the raw data to identify singularities, and in turn avoid the smoothing effect of interpolation. Here, the concentrations of As in samples from the study area are used as an example to examine the differences between the global linear fit and piecewise linear fit methods of singularity estimation.

Zuo et al. (2013) determined that smaller window size intervals should be used for the local analysis of fractal characteristics and anomaly identification, whereas larger window sizes are ideal for use in identifying regional characteristics, but are not ideal for anomaly identification. Hence, in order to reflect and highlight the local and weak anomalies better, this study uses 3 km as the interval of window size to estimate the singularity. In addition, the maximum window size used during this analysis can impact the global linear fitting; as

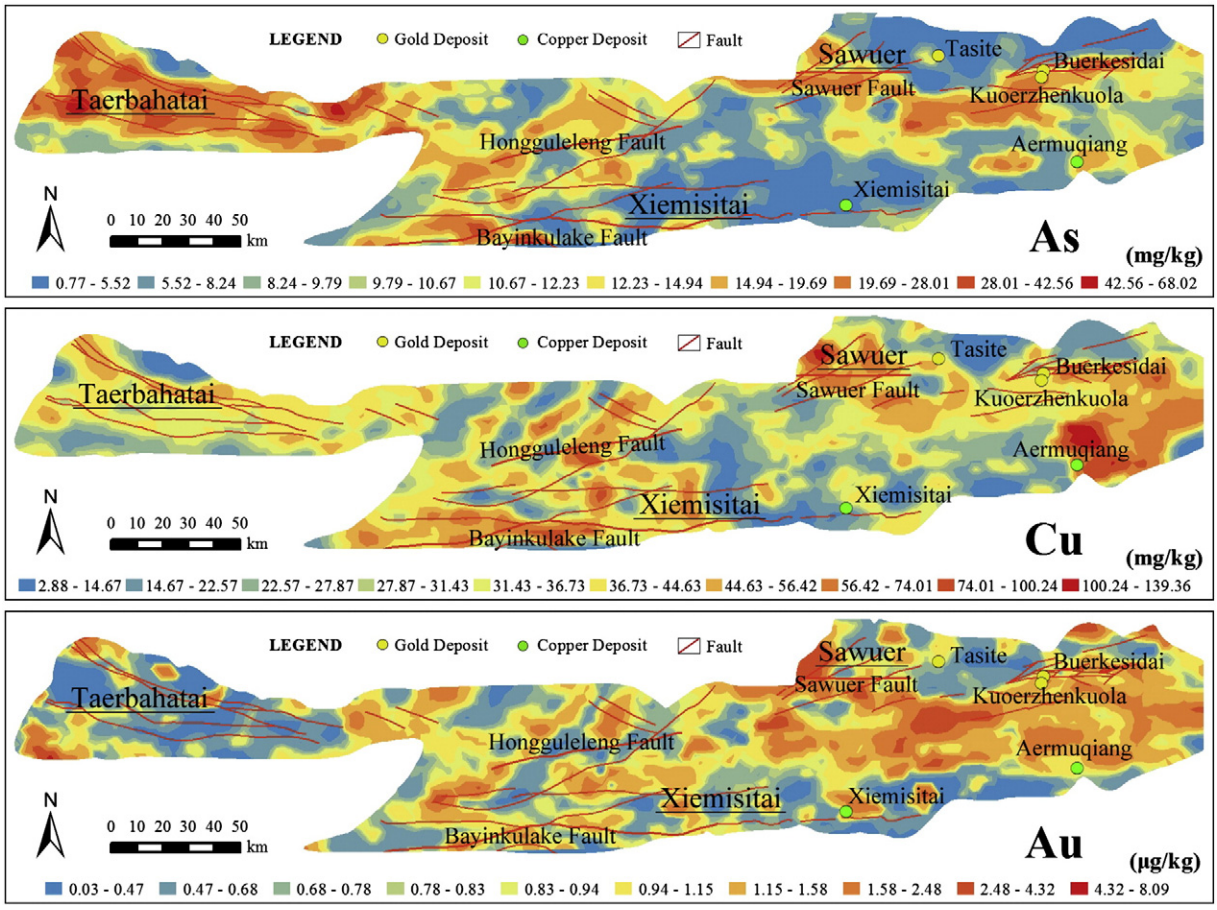

Fig. 9. Maps constructed by multifractal kriging interpolation of As, Cu and Au concentrations, NW Junggar area of northern Xinjiang Province, China.

such, the modelling discussed here compares the singularities identified using two different maximum window sizes (30 and 60 km). Two sets of windows (r_{min} = 3 km, 6 km, 9 km,..., r_{max} = 30 km), (r_{min} = 3 km, 6 km, 9 km,..., r_{max} = 60 km) were used for the global linear fitting and, as the piecewise linear fit method is not greatly influenced by the maximum window size used during the modelling, a maximum window size of 60 km to estimate singularities is used.

The As singularities identified using global linear and piecewise linear fitting methods with different maximum window sizes are shown in Fig. 5. The maximum window size strongly affects the results obtained during linear fitting and, therefore, the location of identified singularities (Fig. 5a, b). The singularities identified using larger maximum window sizes expand the size of the areas that contain elevated concentrations of As, meaning that the data processed using these larger window sizes reflects to some extent regional rather than local geochemical characteristics. In comparison smaller window sizes are more sensitive to local anomalies, and can identify more readily areas with anomalously high As concentrations, supporting the effects of window size variation documented by Zuo et al. (2013).

These data also show that the piecewise linear fitting method (Fig. 5c) can identify more readily local and weak anomalies than the global linear fitting method (Fig. 5a, b). This piecewise approach readily identifies anomalies nearby the Xiemisitai copper and Tasite gold deposits (Fig. 5c), whereas these deposits are not as clearly associated with anomalies within the global linear fit modelling shown in Fig. 5a and b. Given this, the piecewise linear fitting method is used, therefore, with multifractal interpolation to determine the location of Cu and Au singularities; the results of this mapping are shown in Fig. 6.

Fig. 5c shows a good correlation between As singularities and known gold and copper deposits, with all of the known deposits located in the centre or at the edge of areas of As enrichment; there is also high As enrichment approximately along the E–W trending faults within the area. This suggests that faults may be controlling As enrichment. In addition, this modelling approach clearly identifies the Cu singularities associated with known copper deposits in the study area (Fig. 6a). Furthermore, the presence of several areas of anomalously high Au concentration, which means that the wider range in singularity values forms relatively localised areas and singularities with high Au enrichment. Despite this, the anomalies associated with the Kuoerzhenkuola and Buerkesidai gold deposits are still clearly evident within the modelling (Fig. 6a).

5.2. Multifractal kriging interpolation

Ordinary kriging is a linear geostatistical method that is based on a second-order stationary hypothesis (Matheron, 1963). The presence of non-normally distributed data and outliers will decrease the stationarity of the data, whilst increasing fluctuations within variograms, meaning that the presence of real structures within the data may be occluded. The most commonly used method of determining the statistical frequency characteristics of a data set is the Q–Q plot; this approach can determine whether the distribution of the data is normal, lognormal, or neither (Cheng, 2000).

Statistical treatment of the concentrations of As, Cu, and Au within the soil geochemical data set used in this study indicates that none of these elements have normal distributions. In addition, Q–Q plots for log-transformed As, Cu and Au concentrations (Fig. 7) indicate that these data have approximately lognormal distributions, with the exception of a few outliers at high and low concentrations; this type of distribution indicates that these mixed concentrations are controlled by multiple geological events or processes (Zuo et al., 2009). Lognormal kriging is a better approach to the interpolation of lognormally distributed data than ordinary kriging, and is more robust against outliers (Armstrong and Boufassa, 1988); consequently, lognormal kriging was used to plot raster maps for the As, Cu, and Au geochemical data. The structure of the variograms calculated, using these data, was stabilised by deletion of some outliers within the data set, as identified by blue points within Q–Q plots (Fig. 7); this procedure enabled the more accurate identification of spatial variations within the data.

Experimental variograms calculated using the log-transformed data without the excluded outliers shown in Fig. 7 have stable structures and have shapes representative of the spherical model theory. Given this, the spherical variogram model was used to fit the experimental variograms of As, Cu and Au, and the final raster map was produced by lognormal kriging interpolation (Fig. 8).

The concentrations of As within the study area spatially correlate with faults, especially segments of nearly E–W trending faults, and the overall concentration of As is higher in the Taerbahatai area than in the Ximisitai and Sawuer areas (Fig. 8a), indicating also the occurrence of a higher background concentration of As within the Taerbahatai area. In addition, the lognormal kriging interpolation of Cu concentrations (Fig. 8b) indicates a spatial relationship between the Bayinkulake and Hongguleleng faults and areas of anomalously high Cu concentrations; in contrast, the Taerbahatai area is characterised by generally low background concentrations of Cu. The Au kriging map (Fig. 8c) shows that Au concentrations are strongly depleted in the Taerbahatai area, with elevated concentrations localised in the east of the study area and spatially related to locations containing felsic intrusions.

The lognormal kriging interpolation shown in Fig. 8 generally reflects the regional distribution of elements rather than the localised anomalies delineated using singularity identification (Figs. 5 and 6). The large size of the study area means that there may be several differing magmatic and mineralisation-hosting units in this area; the different characteristics of these units mean that they will yield differing soil geochemical background concentrations during weathering. In addition, kriging-based interpolation will also smooth the data, further occluding the presence of both localised and weak anomalies. This

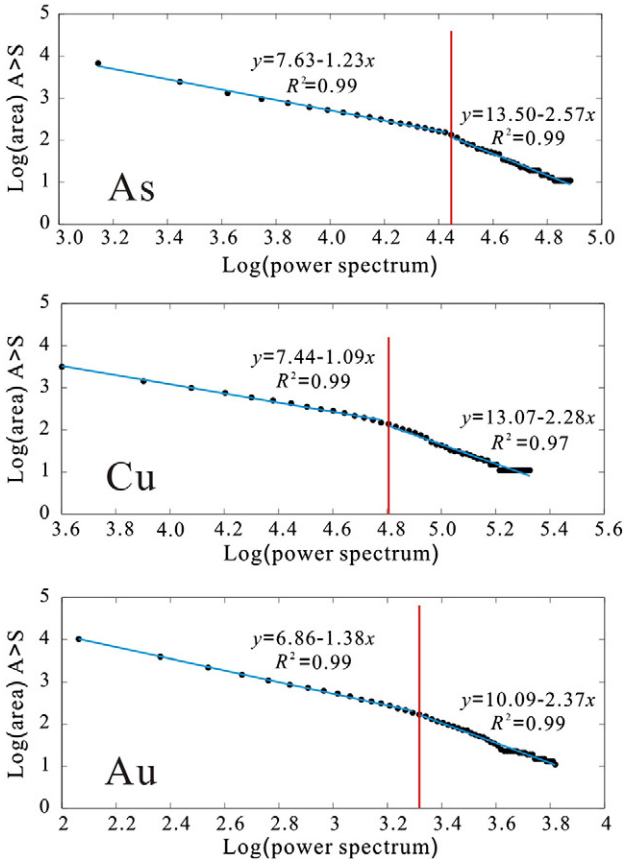

Fig. 10. Log–log plot showing variations in power spectrum (S) versus areas >S ($A > S$) for As, Cu and Au concentration data within the study area.

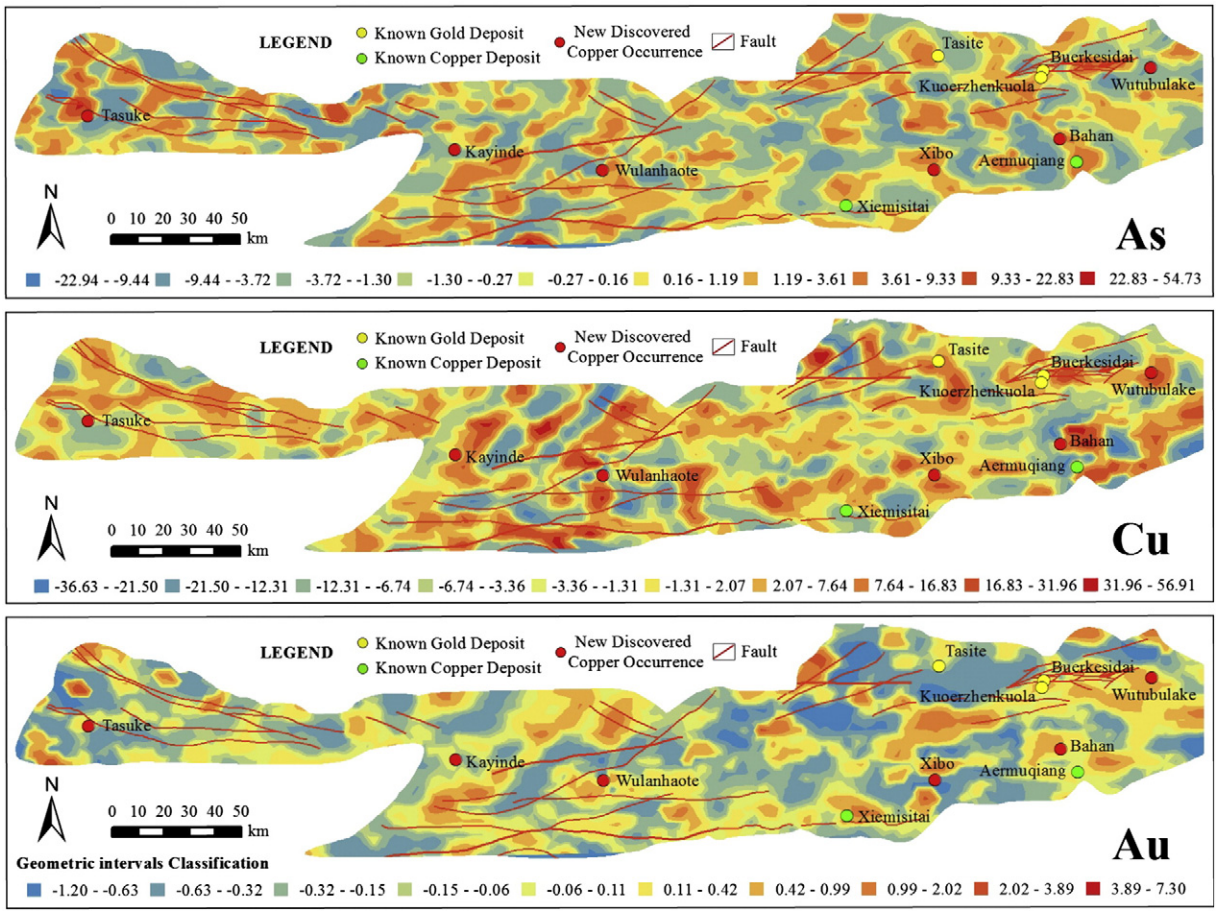

Fig. 11. Maps showing the location of As, Au and Cu geochemical anomalies in the study area determined by S–A fractal modelling compared to the location of known Au and Cu deposits and recently identified Cu prospects, NW Junggar area of northern Xinjiang Province, China.

observation suggests that a combined approach using both kriging interpolation and singularity mapping within a multifractal kriging interpolation method is the best approach to raster mapping of the concentrations of As, Cu and Au in the study area (Fig. 9).

Figs. 8 and 9 indicate that interpolation by multifractal kriging can both enhance localised and weak geochemical anomalies, as well as providing more information on the controls on the regional spatial distribution of the elements of interest than by singularity mapping alone.

5.3. Anomaly separation using S–A fractal modelling

The raster maps produced by interpolation using multifractal kriging (Fig. 9) were transformed to frequency domain data using a Fourier transformation based on a S–A fractal model (Cheng et al., 1994, 2000; Cheng, 2001b, 2006b; Zuo et al., 2013). The fractal characteristics that represent the relationship between the spectral energy density S and the areas $>S$ were then analysed on a log–log plot (Fig. 10).

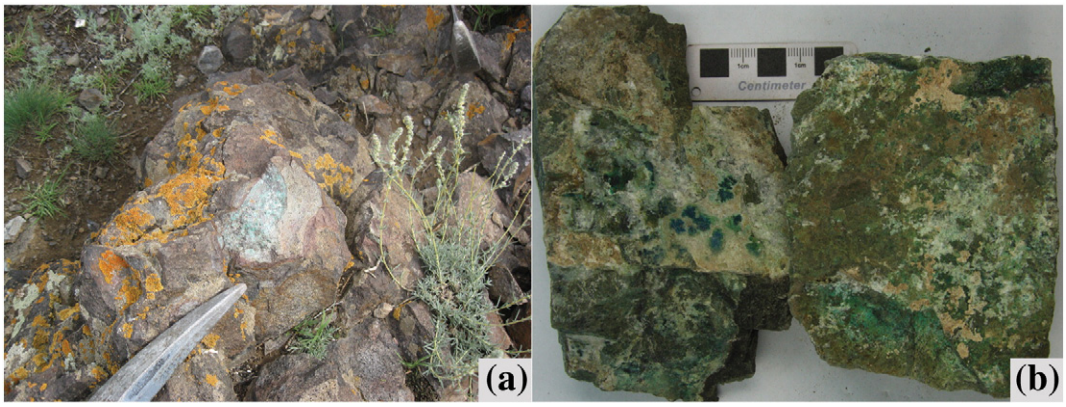

Fig. 12. Photographs from the Bahan copper occurrence: (a) Malachite mineralisation within volcanic breccias; (b) Malachite mineralisation from the Bahan copper occurrence.

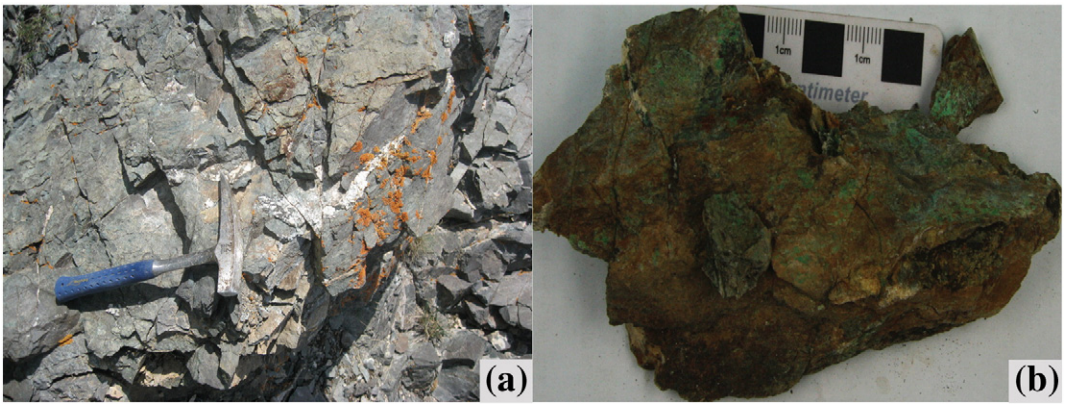

Fig. 13. Photographs from the Wulanhaote copper occurrence: (a) Altered basaltic andesite host of the Wulanhaote occurrence; (b) Malachite mineralisation from the Wulanhaote copper occurrence.

The As, Cu and Au data points shown in Fig. 10 can all be modelled using two straight lines. These lines were fitted using least squares modelling to estimate the parameters of both sections of these straight lines. The cut-off value between these two straight lines was identified, and used to determine anomaly filters for each element. The final stage of this modelling was to use the anomaly filter to separate anomalies and areas with background concentrations before translating these anomalies into spatial domain data (Fig. 11).

The maps produced by S–A fractal modelling shown in Fig. 10 are more useful than the maps produced by multifractal kriging interpolation (Fig. 9) for anomaly identification. The S–A modelling maps especially suppress the influence of the complex background concentrations within the study area, and effectively highlight local anomalies independent of the underlying geology. In addition, the anomalous areas, identified using the S–A fractal model, have more detailed outlines than those delineated by singularity mapping (Figs. 5c and 6), meaning that S–A fractal model derived maps can more accurately target areas for more detailed exploration.

All of the known gold and copper deposits in the study area have coincident As anomalies, identified using the S–A fractal model (Fig. 11a). In comparison, both singularity mapping (Fig. 5c) and kriging and multifractal kriging interpolated raster maps (Figs. 8a and 9a) do not identify high As anomalies associated with the Tasite gold and Xiemisitai copper deposits. Similarly, Cu anomalies detected by using the S–A fractal model have more detailed outlines than those derived by the other methods discussed here, resulting in the identification of a number of local anomalies. These anomalies include the areas around all the known copper deposits in the study area, with the Xiemisitai and Aermutong deposits clearly associated with local Cu anomalies (Fig. 11c). Although there are a number of Au outliers with high concentration, the Au anomaly map produced by S–A fractal modelling can also identify a number of local anomalies. This is exemplified by the weak anomalies in the east of the study area associated with the Kuoerzhenkuola and Buerkesidai gold deposits (Fig. 11b).

The geochemical anomalies shown in Fig. 11 were subsequently ground-truthed by field-based examination and validation, as discussed in Section 6. This ground-truthing directly led to the discovery of a number of mineralised occurrences, indicating that this fractal and multifractal modelling is a highly useful approach to mineral exploration in the study area, and suggests that it could prove useful if applied to other areas.

6. Anomaly ground-truthing and discovery of new mineralised occurrences

The ground-truthing of the S–A fractal modelling-defined As, Cu and Au anomalies shown in Fig. 11 directly led to the discovery of Cu mineralisation in the Bahan and Wulanhaote areas. The Bahan copper occurrence is hosted by mafic volcanic rocks located north of the Aermuqiang copper deposit, and consists of chalcopyrite, malachite, covellite, pyrite, magnetite and haematite mineralisation within a quartz, epidote, chlorite and calcite gangue (Fig. 12). The Wulanhaote copper occurrence is located in the centre of the research area, and is hosted by a basaltic andesite that is cross-cut by a small quartz-bearing syenite intrusion. The mineralisation in the Wulanhaote area includes chalcopyrite, malachite, and pyrite in a quartz, K-feldspar, epidote, chlorite and calcite gangue (Fig. 13).

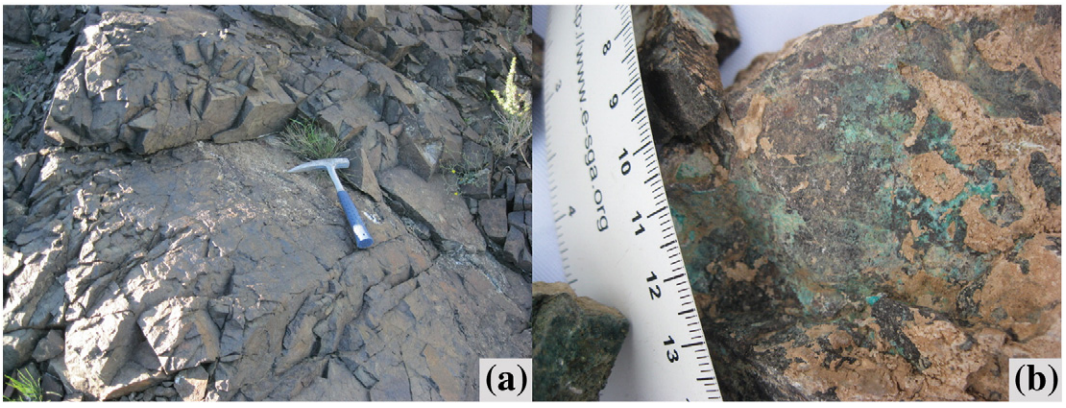

Fig. 14. Photographs of the Xibo copper occurrence: (a) The syenite porphyry host rock for the mineralisation at Xibo; (b) Malachite mineralisation from the Xibo copper occurrence.

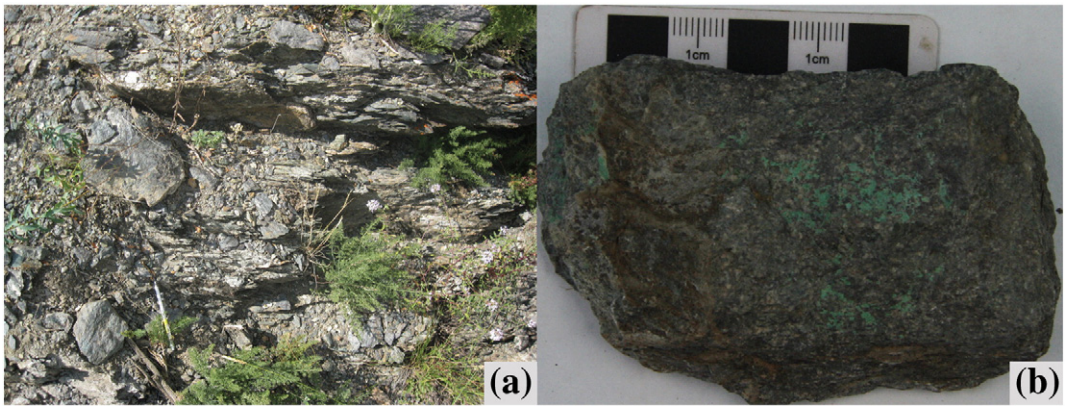

Fig. 15. Photographs of the Kayinde copper occurrence: (a) the basaltic andesite host rock for mineralisation at Kayinde; (b) Malachite mineralisation within a mafic volcanic rock.

Ground-truthing of As and Cu anomalies shown in Fig. 11 also led to the discovery of the Xibo copper and Kayinde copper occurrences. The Xibo copper occurrence is hosted by a basaltic andesite and contains chalcopyrite, pyrite, malachite and magnetite mineralisation associated with quartz and calcite veining and chlorite, epidote and kaolinite alteration (Fig. 14). The Kayinde copper occurrence is similar to the Xibo copper occurrence, and is hosted by a basaltic andesite with a paragenesis of chalcopyrite, pyrite, malachite and magnetite, associated with quartz, epidote, chlorite and calcite gangue minerals (Fig. 15).

In addition to the occurrences outlined above, the investigation of a coincident Cu and Au anomaly (Fig. 11) led to the discovery of the Wutubulake copper occurrence within the Devonian Taerbahatai Group. The copper mineralisation at Wutubulake is hosted by a basaltic andesite and consists of a paragenesis of chalcopyrite, malachite and pyrite, within a quartz, chlorite, epidote and kaolinite gangue (Fig. 16).

The last mineralised occurrence, identified during ground-truthing of the S–A fractal modelling-defined anomalies shown in Fig. 11, is delineated by an As-only anomaly (Fig. 11a). This particular anomaly, surrounded by an area with high background concentrations of As, is associated with the newly discovered Tasuke copper occurrence, which is located within the Tahabahatai area. This area has undergone intense magmatism associated with the intrusion of a series of intermediate to felsic magmas that formed porphyritic pyroxene diorite, granodiorite and granite intrusions and a series of minor mafic dykes. The

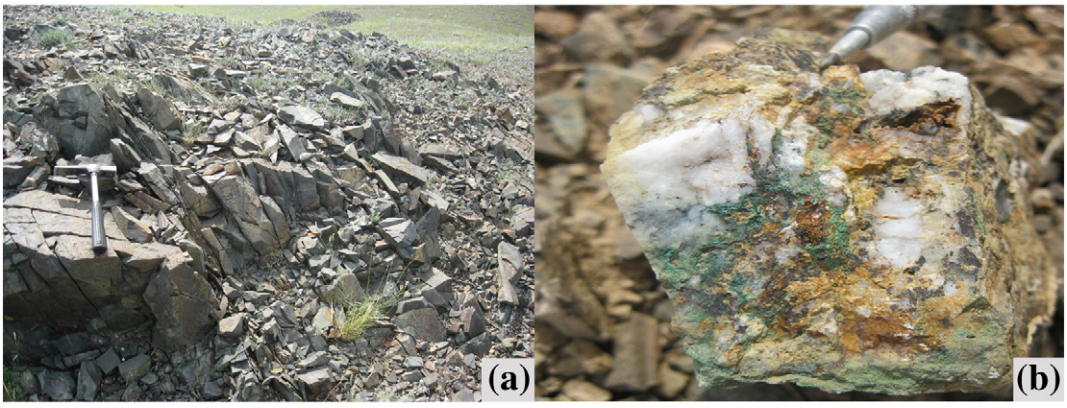

Fig. 16. Photographs of the Wutubulake copper occurrence: (a) The basaltic andesite host rock for mineralisation at Wutubulake; (b) Malachite mineralisation at Wutubulake.

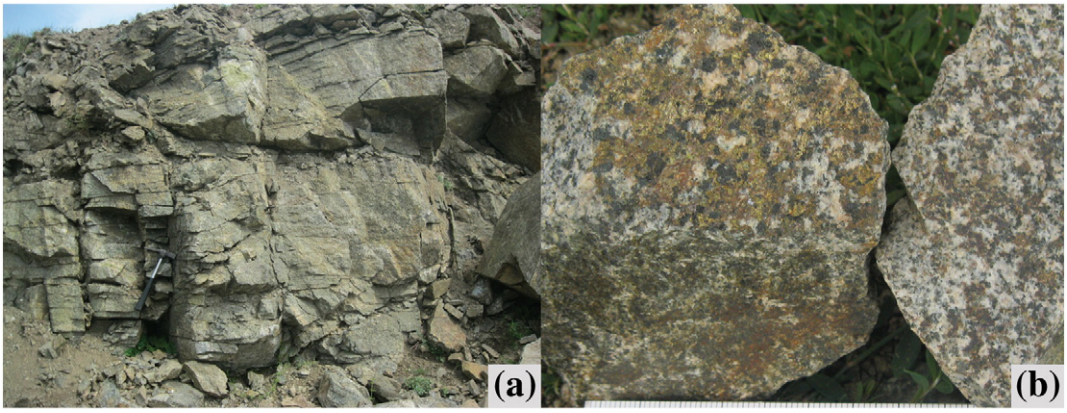

Fig. 17. Photographs of the Tasuke copper mineral occurrence: (a) The granodiorite that hosts the mineralisation at Tasuke; (b) Chalcopyrite mineralisation within granodiorite.

mineralisation at Tasuke is hosted by a granodiorite and consists of chalcopyrite, malachite, magnetite and pyrite, within a quartz, pyroxene, hornblende, plagioclase, K-feldspar, epidote, biotite and calcite gangue (Fig. 17).

This positive ground-truthing and the direct discovery of several new mineralised occurrences is a clear indication of the effectiveness and usefulness of the fractal and multifractal modelling of soil geochemical data during mineral exploration in the study area. These data also indicate that copper mineralisation can be identified by either single or coincident As, Au and Cu anomalies. However, no gold mineralisation was discovered during this ground-truthing, suggesting that further investigation and an improved understanding of the Au anomalies in the study area are needed to ensure the effectiveness of future mineral exploration.

7. Conclusions

The following conclusions were reached about the effective use of fractal and multifractal modelling of soil geochemical data for mineral exploration purposes in the NW Junggar area of northern Xinjiang Province, China:

(1) Improved singularity mapping for identification of soil geochemical anomalies during mineral exploration can be achieved using a piecewise linear fit method; this method also allows localised and weak anomalies, both of which may be related to mineralisation, to be clearly delineated.
(2) An integrated approach that incorporated singularity mapping, interpolation by multifractal kriging and S–A fractal modelling identified a number of distinct anomalies within the NW Junggar area of northern Xinjiang Province, China. All known mineral deposits in this area are associated with distinct geochemical anomalies, and subsequent ground-truthing of anomalies, associated with no known mineralisation, directly led to the identification of a number of previously unknown areas of Cu mineralisation. Further ground-truthing of the anomalies, delineated during this study, may also lead to the identification of additional unidentified mineralised Cu and Au prospects. This suggests that the study area should be considered highly prospective for Cu and Au mineralisation, and in conclusion the use of fractal and multifractal modelling of soil geochemical for mineral exploration proved to be very effective in the study area in the delineation potential Cu and Au mineralization, and the methodology used is considered to be applicable to other areas around the globe.

Acknowledgements

This research was financially supported by funds from the Chinese National Science and Technology Programme during the 12th Five-year Plan Period (Grant No. 2011BAB06B01), the Program for New Century Excellent Talents in University (Grant No. NCET-10-0324) and the China Scholarship Council.

References

Agterberg, F.P., 2012. Multifractals and geostatistics. J. Geochem. Explor. 122, 113–122.
Aitchison, J., 1986. The Statistical Analysis of Compositional Data. Chapman & Hall, London (416 pp.).
Armstrong, M., Boufassa, A., 1988. Comparing the robustness of ordinary kriging and lognormal kriging: outlier resistance. Math. Geol. 20, 447–457.
BGMRXUAR (Bureau of Geology and Mineral Resources of Xinjiang Uygur Autonomous Region), 1993. Regional Geology of Xinjiang Uygur Autonomous Region. Geological Publishing House, Beijing (841 pp. (in Chinese with English abstract)).
Bonham-Carter, G., 1994. Geographic Information Systems for Geoscientists: Modelling with GIS. Elsevier, Oxford (398 pp.).
Buccianti, A., 2015. The FOREGS repository: modelling variability in stream waters on a continental scale revising classical diagrams fromCoDA (compositional data analysis) perspective. In: Demetriades, A., Birke, M., Albanese, S., Schoeters, I., De Vivo, B. (Eds.), Continental. Regional and Local Scale Geochemical Mapping, Special Issue, Journal of Geochemical Exploration 154, pp. 94–104 (this issue).
Carranza, E.J.M., 2009. Geochemical anomaly and mineral prospectivity mapping in GIS. In: Hale, M. (Ed.), Handbook of Exploration and Environmental Geochemistry vol. 11. Elsevier Science Ltd., Oxford (368 pp.).
Chen, J., Han, B., Ji, J., Zhang, L., Zhao, X., He, G., Wang, T., 2010. Zircon U–Pb ages and tectonic implications of Paleozoic plutons in northern West Junggar, North Xinjiang, China. Lithos 115, 137–152 (In Chinese with English abstract).
Cheng, Q., 1999. Multifractality and spatial statistics. Comput. Geosci. 25, 949–961.
Cheng, Q., 2000. Multifractal theory and geochemical element distribution pattern. Earth Sci. J. China Univ. Geosci. 25, 311–318 (In Chinese with English abstract).
Cheng, Q., 2001a. Multifractal and geostatistic methods for characterizing local structure and singularity properties of exploration geochemical anomalies. Earth Sci. 26, 161–164.
Cheng, Q., 2001b. Spatial self-similarity and geophysicl and geochemical anomaly decomposition. Prog. Geophys. 16, 8–17.
Cheng, Q., 2006a. Singularity-generalized self-similarity-fractal spectrum (3S) models. Earth Sci. J. China Univ. Geosci. 31, 42–53 (In Chinese with English abstract).
Cheng, Q., 2006b. Multifractal modelling and spectrum analysis: methods and applications to gamma ray spectrometer data from southwestern Nova Scotia, Canada. Sci. China Ser. D Earth Sci. 49, 283–294.
Cheng, Q., 2007. Mapping singularities with stream sediment geochemical data for prediction of undiscovered mineral deposits in Gejiu, Yunnan Province, China. Ore Geol. Rev. 32, 314–324.
Cheng, Q., 2008a. Non-linear theory and power-law models for information integration and mineral resources quantitative assessments, progress in geomathematics. In: Bonham-Carter, G.F., Cheng, Q. (Eds.), Progress in Geomathematics. Springer-Verlag. Berlin, Heidelberg, pp. 195–225.
Cheng, Q., 2008b. A combined power-law and exponential model for streamflow recessions. J. Hydrol. 352, 157–167.
Cheng, Q., 2008c. Modeling local scaling properties for multiscale mapping. Vadose Zone J. 7, 525–532.
Cheng, Q., 2012. Singularity theory and methods for mapping geochemical anomalies caused by buried sources and for predicting undiscovered mineral deposits in covered areas. J. Geochem. Explor. 122, 55–70.
Cheng, Q., Agterberg, F.P., 2009. Singularity analysis of ore-mineral and toxic trace elements in stream sediments. Comput. Geosci. 35, 234–244.
Cheng, Q., Agterberg, F., Ballantyne, S., 1994. The separation of geochemical anomalies from background by fractal methods. J. Geochem. Explor. 51, 109–130.
Cheng, Q., Xu, Y., Grunsky, E., 2000. Integrated spatial and spectrum method for geochemical anomaly separation. Nat. Resour. Res. 9, 43–52.
Cheng, Q., Xia, Q., Li, W., Zhang, S., Chen, Z., Zuo, R., Wang, W., 2010. Density/area power-law models for separating multi-scale anomalies of ore and toxic elements in stream sediments in Gejiu mineral district, Yunnan Province, China. Biogeosci. Discuss. 7, 4273–4293.
Clark, I., 1979. Practical Geostatistics. Applied Science Publishers, London (119 pp.).
Clark, I., Harper, W.V., 2007. Practical Geostatistics 2000. Geostokos (Ecosse) Ltd., Scotland (412 pp.).
Egozcue, J.J., Pawlowsky-Glahn, V., 2011. Basic concepts and procedures. Chapter 2. In: Pawlowsky-Glahn, V., Buccianti, A. (Eds.), Compositional Data Analysis: Theory and Applications. John Wiley & Sons Ltd., Chichester, U.K., pp. 12–28.
Fan, Y., Zhou, T., Yuan, F., Tan, L., Cooke, D., MEFFRE, S., Yang, W., He, L., 2007. LA-ICP MS zircon age of Tasite pluton in Sawuer region of west Junggar, Xinjiang. Acta Petrol. Sin. 23, 1901–1908 (In Chinese with English abstract).
Filzmoser, P., Hron, K., Reimann, C., 2009. Univariate statistical analysis of environmental (compositional) data — problems and possibilities. Sci. Total Environ. 407, 6100–6108.
Filzmoser, P., Hron, K., Reimann, C., 2010. The bivariate statistical analysis of environmental (compositional) data. Sci. Total Environ. 408, 4230–4238.
Filzmoser, P., Reimann, C., Birke, M., 2014. Univariate data analysis and mapping. Chapter 8. In: Reimann, C., Birke, M., Demetriades, A., Filzmoser, P., O'Connor, P. (Eds.), Chemistry of Europe's Agricultural Soils — Part A. Geologisches Jahrbuch (Reihe B102), Schweizerbarth, Hannover, pp. 67–81.
Guo, D.L., 1997. Tectono-metallogenetic mechanism for the Buerkesidai gold deposit. Geotecton. Metallog. 21, 162–166 (In Chinese with English abstract).
Isaaks, E.H., Srivastava, R.M., 1990. An Introduction to Applied Geostatistics. Oxford University Press, Oxford, U.K. (561 pp.).
Jahn, B.-M., Wu, F., Chen, B., 2000. Granitoids of the Central Asian Orogenic Belt and continental growth in the Phanerozoic. Trans. R. Soc. Edinb. Earth Sci. 91, 181–194.
Journel, A.G., Huijbreghts, Ch.J., 1978. Mining Geostatistics. Academic Press, London (600 pp.).
Krige, D., 1951. A statistical approach to some basic mine evaluation problems on the Witwateround. J. Chem. Metall. Min. Soc. S. Afr. 52, 119–139.
Li, Q., 2005. Multifractal-krige interpolation method. Adv. Earth Sci. 20, 248–255.
Lima, A., De Vivo, B., Cicchella, D., Cortini, M., Albanese, S., 2003. Multifractal IDW interpolation and fractal filtering method in environmental studies: an application on regional stream sediments of (Italy), Campania region. Appl. Geochem. 18, 1853–1865.
Matheron, G., 1963. Principles of geostatistics. Econ. Geol. 58, 1246–1266.
Pan, G., Harris, D.P., 2000. Information Synthesis for Mineral Exploration. Oxford University Press, New York (461 pp.).
Reimann, C., Filzmoser, P., Fabian, K., Hron, K., Birke, M., Demetriades, A., Dinelli, E., Ladenberger, A., The GEMAS Project Team, 2012. The concept of compositional data analysis in practice — total major element concentrations in agricultural and grazing land soils of Europe. Sci. Total Environ. 426, 196–210.
Sadeghi, M., Billay, A., Carranza, E.J.M., 2015. Analysis and mapping of soil geochemical anomalies: implications for bedrock mapping and gold exploration in Giyani area,

South Africa. In: Demetriades, A., Birke, M., Albanese, S., Schoeters, I., De Vivo, B. (Eds.), Continental. Regional and Local Scale Geochemical Mapping, Special Issue, Journal of Geochemical Exploration 154, pp. 180–193 (this issue).
Shen, P., Shen, Y., Liu, T., Li, G., Zeng, Q., 2007. Genesis of volcanic-hosted gold deposits in the Sawur gold belt, northern Xinjiang, China: evidence from REE, stable isotopes, and noble gas isotopes. Ore Geol. Rev. 32, 207–226.
Shen, P., Shen, Y., Tie-bing, L., Pan, H.-D., Meng, L., Song, G., Dai, H., 2010. Discovery of the Xiemisitai copper deposit in western Junggar, Xinjiang and its geological significance. Xinjiang Geol. 28, 413–418 (In Chinese with English abstract).
Wang, J., Wang, Y., Wang, L., 2004. The Junggar immature continental crust province and its mineralization. Acta Geol. Sin. 78, 337–344 (In Chinese with English abstract).
Wang, W., Zhao, J., Cheng, Q., 2011. Analysis and integration of geo-information to identify granitic intrusions as exploration targets in southeastern Yunnan District, China. Comput. Geosci. 37, 1946–1957.
Yin, Y., Chen, D., An, Y., Li, J., Fan, Y., You, Z., Yang, J., 1996. Characteristics of the Kuoerzhenkuola epithermal gold deposit in Sawuershan, Xinjiang. Geol. Explor. Nonferrous Met. 5, 278–283 (In Chinese with English abstract).
Yuan, F., Li, X., Jowitt, S.M., Zhang, M., Jia, C., Bai, X., Zhou, T., 2012. Anomaly identification in soil geochemistry using multifractal interpolation: a case study using the distribution of Cu and Au in soils from the Tongling mining district, Yangtze metallogenic belt, Anhui province, China. J. Geochem. Explor. 116–117, 28–39.
Zhang, R., 2005. The Theory and Application of Spatial Variation. Science Press, BeiJing (188 pp.).
Zhou, T., Yuan, F., Tan, L., Fan, Y., Yue, S., 2006. Geodynamic significance of the A-type granites in the Sawuer region in west Junggar, Xinjiang: Rock geochemistry and SHRIMP zircon age evidence. Sci. China Earth Sci. 29, 113–123.
Zuo, R., 2011a. Decomposing of mixed pattern of arsenic using fractal model in Gangdese belt, Tibet, China. Appl. Geochem. 26, 271–273.
Zuo, R., 2011b. Identifying geochemical anomalies associated with Cu and Pb–Zn skarn mineralization using principal component analysis and spectrum–area fractal modeling in the Gangdese Belt, Tibet (China). J. Geochem. Explor. 111, 13–22.
Zuo, R., Cheng, Q., 2008. Mapping singularities—a technique to identify potential Cu mineral deposits using sediment geochemical data, an example for Tibet, west China. Mineral. Mag. 72, 531–534.
Zuo, R., Cheng, Q., Agterberg, F., Xia, Q., 2009. Application of singularity mapping technique to identify local anomalies using stream sediment geochemical data, a case study from Gangdese, Tibet, western China. J. Geochem. Explor. 101, 225–235.
Zuo, R., Carranza, E.J.M., Cheng, Q., 2012. Fractal/multifractal modelling of geochemical exploration data. J. Geochem. Explor. 122, 1–3.
Zuo, R., Xia, Q., Zhang, D., 2013. A comparison study of the C–A and S–A models with singularity analysis to identify geochemical anomalies in covered area. Appl. Geochem. 33, 165–172.
Zuo, R., Wang, J., Chen, G., Yang, M., 2015. Identification of weak anomalies: amultifractal perspective. In: Demetriades, A., Birke, M., Albanese, S., Schoeters, I., De Vivo, B. (Eds.), Continental. Regional and Local Scale Geochemical Mapping, Special Issue, Journal of Geochemical Exploration 154, pp. 200–212 (this issue).